Tetrahedron 70 (2014) 6229–6234

Contents lists available at ScienceDirect

Tetrahedron

journal homepage: www.elsevier.com/locate/tet

Design and characterization of Bodipy derivatives for bulk heterojunction solar cells

Safacan Kolemen [a], Yusuf Cakmak [a], Tugba Ozdemir [a], Sule Erten-Ela [b], Muhammed Buyuktemiz [c], Yavuz Dede [c], Engin U. Akkaya [a,d,*]

[a] UNAM-Institute of Materials Science and Nanotechnology, Bilkent University, Ankara 06800, Turkey
[b] Institute of Solar Energy, Ege University, Izmir 35100, Turkey
[c] Department of Chemistry, Gazi University, Ankara 06500, Turkey
[d] Department of Chemistry, Bilkent University, Ankara 06800, Turkey

ARTICLE INFO

Article history:
Received 27 December 2013
Received in revised form 4 March 2014
Accepted 14 March 2014
Available online 25 March 2014

Keywords:
Bulk heterojunction solar cells
Bodipy
Near-IR sensitizers
Panchromaticity
Conversion efficiency

ABSTRACT

Two electron rich Bodipy dyes with strong absorptivities in the visible region were designed and synthesized as potential electron donors in bulk heterojunction photovoltaic constructs. Overall efficiency is above 1%, with impressive responsiveness at both UV and near-IR ends of the visible spectrum. Computational studies reveal an unexpected effect of *meso*-substituents on the electron transfer efficiency.

1. Introduction

Bulk heterojunction (BHJ) organic photovoltaic (OPV) technologies are recognized as a promising alternative to traditional liquid electrolyte based dye-sensitized solar cells (DSSCs) following the improved conversion efficiencies during the last decade.[1] In these all-organic cells, electron donor/acceptor moieties are blended together in the photoactive layer and conductive polymers (PEDOT:PSS/polyethylenedioxythiophene:polystyrene sulfonate) are incorporated as replacement to inorganic semi-conductors.[2] BHJ-OPV offers a promising modality towards solvent free, large area, reduced weight, and environmentally friendly OPV constructs.

Common strategy for the fabrication of BHJ-OPV is to combine fullerene derivatives as an electron acceptor (in most cases phenyl-C60/61/70-butryic acid methyl ester; PCBM) with conjugated polymers as electron donors.[1c,2] Conjugated polymers, with their high film forming qualities, resulted in moderate to high efficiencies.[3] However, challenging synthetic problems, structural concerns and purification problems generate a clear impetus to find substitutes for the polymeric component of the photovoltaic cell. Another important issue with the polymers is their large optical band gaps. This causes polymer to mostly absorb at high-energy part of the electromagnetic spectrum within a very narrow wavelength range. Thus, significant effort has been placed to find longer wavelength absorbing polymers.[4] On the other hand, as a reasonable alternative, more suitable smaller molecules were also employed as donors.[5] Among the possible donor molecules, Boradiazaindacene (also known as Bodipy)[6] dyes appear to be promising candidates due to their tunable absorption spectra with high extinction coefficients, multiple modification sites amenable for derivatization, photostability, ease of synthesis and relatively long excited state lifetimes.[7] Bodipy dyes have been widely used in biological labeling and molecular sensors,[8] as sensitizers for photodynamic therapy,[9] energy transfer cassettes and light harvesting,[10] and in logic gates studies.[11] Besides these applications, as a result of their suitable characteristics, Bodipy dyes were also employed in liquid electrolyte,[12] solid state[13] and BHJ-OPV[14] solar cells.

In this work, we revisited the rich Bodipy chemistry and designed two near-IR absorbing donor molecules (**BHJ 1** & **BHJ 2**) to investigate their photovoltaic performance in BHJ-OPV (Fig. 1). The main goal was to obtain panchromatic sensitization by including near-IR absorption.

* Corresponding author. Tel.: +90 312 290 3570; fax: +90 312 266 4365; e-mail address: eua@fen.bilkent.edu.tr (E.U. Akkaya).

0040-4020/$ – see front matter © 2014 Elsevier Ltd. All rights reserved.
http://dx.doi.org/10.1016/j.tet.2014.03.049

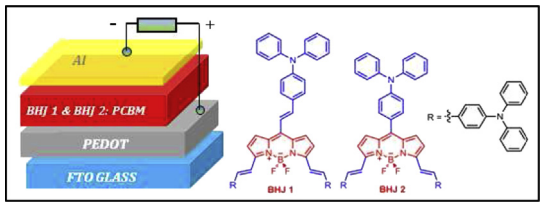

Fig. 1. Structures of sensitizers **BHJ 1** & **BHJ 2** and schematic representation of the BHJ-OPV cell.

2. Results and discussion

Our previous Bodipy sensitizers[12d] clearly showed that the absence of methyl groups on positions 1 and 7 has a positive effect on extended conjugation and favors the electron transfer processes. This is the result of smaller dihedral angle between *meso*-phenyl moieties and the Bodipy core.

In the design of **BHJ 1**, we are not just removing those methyl groups, but also linking the electron donor diphenylamino phenyl moiety at *meso* position with a styryl unit in order to further improve the conjugation and flexibility within the sensitizer. *meso*-Phenyl substituted analogue of **BHJ 2** was also studied to observe the effect of structural modifications on efficiency of the donor. As a final design requirement, additional diphenylamino phenyl groups were incorporated at the 3 and 5 positions of the Bodipy in both **BHJ 1** & **2** to obtain near-IR absorbing dyes and stronger electron donating sensitizers.

BHJ 1 and **BHJ 2** were synthesized according to established protocols. In the case of **BHJ 1** standard Bodipy synthesis procedure with acetyl chloride and 2-methyl pyrrole was applied. In the synthesis of **BHJ 2**, another approach was taken, making use of the reaction of diphenylaminobenzaldehyde and 2-methyl pyrrole. Once the desired Bodipy cores were constructed, targeted compounds were obtained by Knoevenagel condensation reactions in the presence of piperidine and acetic acid.

Photophysical and electrochemical characterization data of the sensitizers in solution are listed in Tables 1 and 2. Electronic absorption spectra (Fig. 2 top) of both dyes show strong and broad ($S_0 \rightarrow S_1$) absorption bands in the red and near-IR region of the spectrum with high extinction coefficients. As expected, extended conjugation in **BHJ 1** result in red-shifted peak centered around 748 nm. Very low fluorescence intensity ($\phi_f \approx 1\%$) of **BHJ 1** can be attributed to the rotation of the double bond around the dihedral axis in the excited state. More rigid **BHJ 2** on the other hand, shows

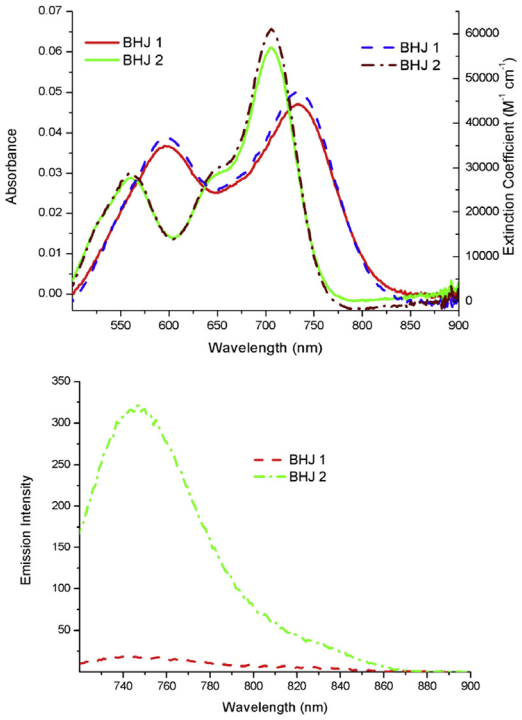

Fig. 2. (top) Electronic absorption and (bottom) emission spectra of **BHJ 1** (red & blue) and **BHJ 2** (green & dark red) in $CHCl_3$.

clear emission peak around 750 nm (Fig. 2 bottom) with moderate fluorescence quantum yield ($\phi_f \approx 24\%$).

Cyclic voltammetry data (CV) were acquired in chloroform (10^{-3} M). A three-electrode cell was used consisting of glassy carbon supporting electrode, platinum wire counter electrode, and Ag/AgCl reference electrode. Data were taken with ferrocene as the internal reference electrode. CV spectra (Fig. 3) of sensitizers show both reversible oxidation and reduction peaks (Table 2). The lowest unoccupied molecular (LUMO) energy of **BHJ 1** and **BHJ 2** are −3.59 and −3.42 eV, respectively. LUMO energies of dyes are clearly higher than the LUMO energy of PCBM (≈−3.90 eV), which suggests an efficient electron transfer from excited donor to acceptor PCBM. Another remarkable result of the CV study is that the highest occupied molecular orbital (HOMO) energy levels of the sensitizers are deeper than the commonly used P3HT (poly(3-hexylthiophene-2,5-diyl)) conjugated polymer[16] suggesting an improved oxidative stability for **BHJ 1** and **2**.

Table 1
Photophysical characterization of **BHJ 1** and **2**

Dye	λ_{abs}/(nm)[a]	ε_{max}/(M^{-1} cm^{-1})[a]	λ_{ems}/(nm)[a]	ϕ_f/(%)[b]
BHJ 1	748	37,000	755	1
BHJ 2	710	46,000	750	24

[a] Data were acquired in $CHCl_3$.
[b] Reference compound: tetrastyryl dye 2 in Ref. 15 (ϕ_f=42%) in $CHCl_3$.

Table 2
Photophysical and electrochemical characterization of **BHJ 1** and **2**

Dye	E_{ox}/(V)[a]	E_{red}/(V)[a]	E_{HOMO}/(eV)[a]	E_{LUMO}/(eV)[a]	$E_{band\ gap}$/(eV)[a]
BHJ 1	0.60	−0.82	−5.00	−3.59	1.41
BHJ 2	0.58	−0.97	−4.96	−3.42	1.54

[a] Solutions were prepared in $CHCl_3$ (10^{-3} M).

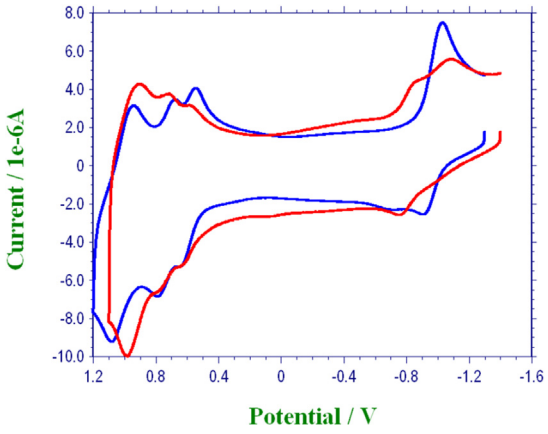

Fig. 3. Cyclic voltammograms of **BHJ 1** (red) and **BHJ 2** (blue).

Film making properties and morphology of organic materials are another important factors for organic photovoltaic devices. The surface morphology of thin films of BHJ solar cells was investigated by atomic force microscopy (AFM) in non-contact mode (see ESD). AFM results show that **BHJ 1** makes more homogenous and thinner film with less roughness.

Bulk heterojunction solar cells were fabricated with the device architecture FTO/PEDOT:PSS/**BHJ 1**/**2**:$PC_{61}BM$/Al (Fig. 1). The Bodipy/$PC_{61}BM$ blend ratio was 1:2 for both sensitizers. First step of the photovoltaic characterization was to acquire current/voltage plots (Fig. 4 top). Device performances were characterized under AM 1.5 G condition with illumination intensity of 100 mW/cm^2 using a solar simulator (Table 3). **BHJ 1** has higher overall conversion efficiency (η=1.50) with 7.00 mA/cm^2 short-circuit photo-current density (J_{sc}) than **BHJ 2** (η=0.36, J_{sc}=2.86 mA/cm^2).

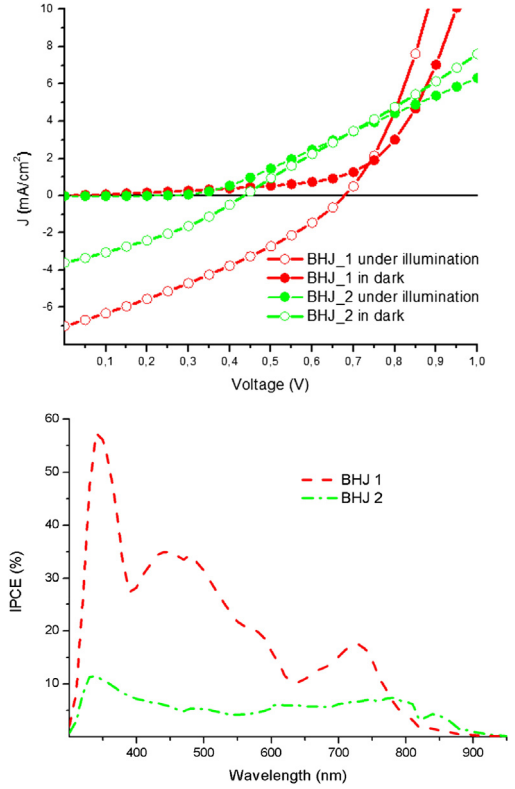

Fig. 4. Top: Current versus voltage (*J*/*V*) plots of the sensitizers. Bottom: Incident photon to current efficiency (IPCE) plots as a function of wavelength for Bodipy based BHJ-OPVs.

Table 3
BHJ-OPV performance parameters of Bodipy dyes

Dye	V_{oc}[a]/mV	J_{sc}[a]/mA cm^{-2}	ff[a]	η[a]/%
BHJ 1	680	7.00	0.31	**1.50**
BHJ 2	430	3.59	0.32	**0.51**

[a] V_{oc} is the open-circuit voltage, J_{sc} is the short-circuit current, ff is the fill factor and η is the overall conversion efficiency of the bulk heterojunction cell under AM 1.5 G condition with an illumination intensity of 100 mW/cm^2 using a solar simulator.

Fig. 4 (bottom) represents the IPCE plots as a function of wavelength. Curves for both sensitizers are essentially flat enough between 350 and 800 nm to satisfy the panchromaticity goal. In addition to that **BHJ 1** has approximately 20% of incident photon to current efficiency around 700 nm. This is a highly noteworthy result for such long wavelengths. IPCE plots are in correlation with J/V curves and thin film absorption spectra (see ESD), in which **BHJ 1** has a better response. It is important to note that excited state characteristics of dyes have direct influence on the electron transfer efficiency. Significant emission of **BHJ 2** ($\phi_f \approx 24\%$) suggests that fluorescence degradation pathways decrease the efficiency of electron transfer from dye to fullerene. On the other hand, in the case of almost non-emissive dye **BHJ 1** ($\phi_f \approx 1\%$) electrons in the excited state might have mostly directed to the acceptor due to restricted relaxation alternatives. This can be attributed as one of the reasons for the overall conversion efficiency differences.

Further insight into somewhat different device performances of **BHJ 1** and **BHJ 2** was obtained by theoretical studies. Our computations aimed to establish an electronic structure rationale for: (i) Why excitation of the dye in the bulk yields photo-current generation? and (ii) What key features are responsible for the different efficiencies of **BHJ 1** and **2**?

In accordance with the experimental blend ratio (2:1 for fullerene/dye) we constructed the super-molecule depicted in Fig. 5 and carried a full geometry optimization. At the optimal dye–fullerene distance (at a separation of 7 and 8 Å measured from the fullerene center for **BHJ 1** and **2**, respectively, see ESD) both dyes undergo a Bodipy→Fullerene type of charge transfer (CT) as shown in Fig. 5. The nearest distances of the dye planes to fullerene are calculated to be 5.0 and 4.8 Å for **BHJ 1** and **2**, respectively. The analogous distance for the truncated system however is 3.3 Å, which is in excellent agreement with the previously reported[17] values around 3.5 Å for essentially planar dyes (Fig. 5). Thus the *meso*-substituents on Bodipy that assume a non-coplanar arrangement (Fig. S15), dictate a longer dye–fullerene distance than the generally observed stacking distance of ca. 3.5 Å.

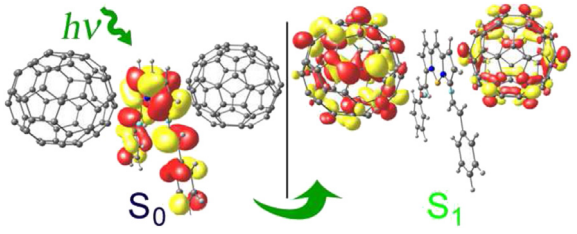

Fig. 5. Computed primary constituents of the $S_0 \rightarrow S_1$ excitation. This simplified picture illustrates the excitation character of both blends.

The molecular orbitals participating in the excitation process are clearly localized on the donor and acceptor moieties. This picture perfectly correlates with the photo-induced electron transfer to the fullerene, however different efficiencies of the dyes need clarification.

A closer inspection of the structural properties of the two dyes reveal that *meso*-substituents are situated at significantly different dihedral angles (**BHJ 1** 35° vs **BHJ 2** 50°) with respect to the Bodipy core (See ESD). This observation led us to study the effect of proximity of fullerene to the Bodipy core on the excitation process. Rotation of the *meso*-substituent (in the energetically allowed region—see ESD) results in differences in dye–Ful. distance, which remarkably effects the strength of CT as the oscillator strength decreases ca. 20-fold upon departure of the acceptor (Fig. 6). Density Functional calculations verify the dye→Ful. CT process and suggest that the structural clash originating from the more twisted *meso*-substituent in **BHJ 2** is responsible for a decreased communication between donor and acceptor moieties eventually decreasing the device efficiency. Consequently, electronic structure analyses reveal that an optimum dye–acceptor distance (that could be predicted by studying the computed oscillator strengths) is another key parameter in enhancing the device efficiency and synthetic strategies in designing substituents for tuning the core properties of the dye should be shaped accordingly.

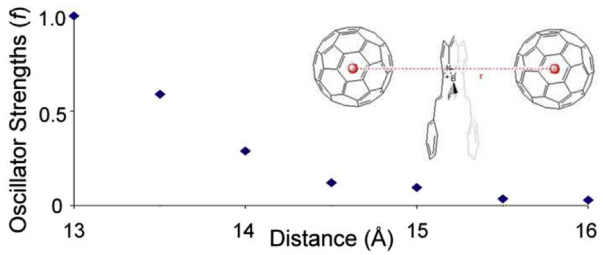

Fig. 6. Relative normalized oscillator strengths (f) in the $S_0 \rightarrow S_1$ excitation for different dye–Ful. distances.

3. Conclusion

In conclusion, bulk heterojunction photovoltaics clearly require optimization of multiple parameters; electronic structure and bulk properties of the donor compounds are both important. Considering the fact that Bodipy dyes show an impressive performance, especially at the long wavelength region of the visible spectrum, it is also evident that these versatile dyes are very promising candidates as panchromatic dyes and electron donors.

4. Experimental

4.1. Materials

All chemicals and solvents obtained from suppliers were used without further purification. Reactions were monitored by thin layer chromatography using Merck TLC Silica gel 60 F_{254}. Chromatography on silica gel was performed over Merck Silica gel 60 (particle size: 0.040–0.063 mm, 230–400 mesh ASTM). Synthetic pathways for all compounds are given in Fig. 7.

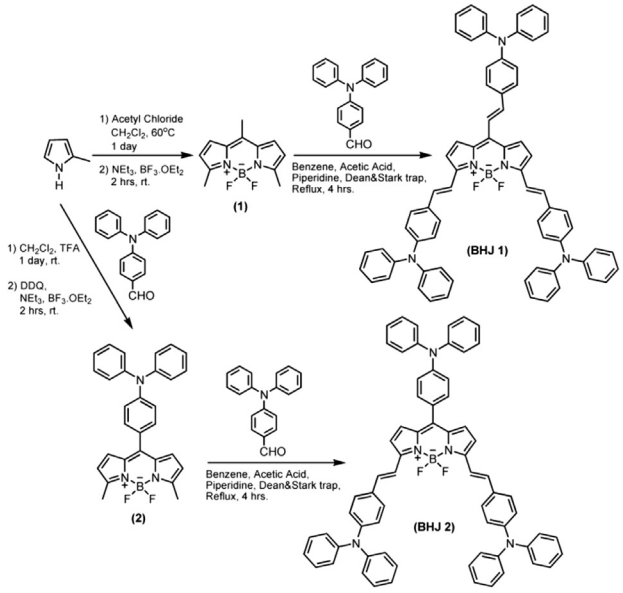

Fig. 7. Synthesis of **BHJ 1** & **BHJ 2**.

4.2. Characterization

^{1}H NMR and ^{13}C NMR spectra were recorded at room temperature on Bruker DPX-400 (operating at 400 MHz for ^{1}H NMR and 100 MHz for ^{13}C NMR) in $CDCl_3$ with tetramethylsilane (TMS) as internal standard. Coupling constants (J values) are given in Hertz and chemical shifts are reported in parts per million (ppm). Splitting patterns are designated as s (singlet), d (doublet), t (triplet), q (quartet), m (multiplet), and p (pentet). Absorption spectra were acquired using a Varian Cary-100 spectrophotometer. Fluorescence spectra were determined on a Varian Eclipse spectrofluorometer. Excitation slit was set at 5 nm and emission slit was set at 5 nm. Mass spectra were recorded on Agilent Technologies 6530 Accurate-Mass Q-TOF LC/MS. Spectrophotometric grade solvents were used for spectroscopy experiments.

4.3. Synthetic details

*4.3.1. Synthesis of (**1**).* To a 1 L round-bottomed flask containing 400 mL argon-degassed CH_2Cl_2 were added 2-methyl pyrrole (8.41 mmol, 1.035 g) and acetyl chloride (3.5 mmol, 1.0 g). The reaction mixture was refluxed overnight at 60 °C. 5 mL of Et_3N and 5 mL of $BF_3 \cdot OEt_2$ were successively added and after 30 min, the reaction mixture was washed three times with water (3×100 mL), which was then extracted into the CH_2Cl_2 (3×100 mL) and dried over anhydrous Na_2SO_4. The solvent was evaporated and the residue was purified by silica gel column chromatography using CH_2Cl_2 as the eluant. Dark red solid (606.9 mg, 31%). ^{1}H NMR (400 MHz, $CDCl_3$): δ=7.05 (d, J=4.12, 2H), 6.35 (d, J=4.12, 2H), 2.60 (s, 6H), 2.39 (s, 3H). ^{13}C NMR (100 MHz, $CDCl_3$): δ_C 156.7, 140.1, 135.0, 126.9, 122.3, 118.8, 118.7, 118.6, 15.2, 14.7. ESI-MS: m/z: calcd: 234.11399, found: 234.11004 $[M-H]^+$, Δ=16.8 ppm.

*4.3.2. Synthesis of BHJ **1**.* (**1**) (0.43 mmol, 100 mg) and *N*,*N*-diphenylaminobenzaldehyde (1.50 mmol, 204.68 mg) were added to a 100 mL round-bottomed flask containing 50 mL benzene and to this solution was added piperidine (0.5 mL) and acetic acid (0.5 mL). The mixture was heated under reflux by using a Dean Stark trap and reaction was monitored by TLC (2:1 EtOAc/Hexane). When all the starting material had been consumed, the mixture was cooled to room temperature and solvent was evaporated. Water (100 mL) added to the residue and the product was extracted into the CH_2Cl_2 (3×100 mL). Organic phase dried over Na_2SO_4, evaporated and residue was purified by silica gel column chromatography using (2:1 EtOAc/Hexane) as the eluant. Black solid (60 mg, %25). ^{1}H NMR (400 MHz, $CDCl_3$): δ=7.70 (d, J=16.32, 2H), 7.51 (d, J=8.60, 4H), 7.49 (d, J=1.24, 2H), 7.35–7.20 (m, 14H), 7.19–7.07 (m, 28H), 6.90 (d, J=3.0, 2H). ^{13}C NMR (100 MHz, $CDCl_3$): δ_C 153.5, 149.3, 148.6, 147.2, 147.0, 140.6, 135.2, 135.1, 130.5, 129.7, 129.5, 129.4, 128.6, 128.5, 126.0, 125.2, 123.9, 123.6, 122.5, 122.2, 119.6, 117.8, 115.3 ppm. ESI-MS: m/z: calcd: 999.42838, found: 999.43313 $[M-H]^+$, Δ=4.75 ppm.

*4.3.3. Synthesis of (**2**).* To a 1 L round-bottomed flask containing 400 mL argon-degassed CH_2Cl_2 were added 2-methyl pyrrole (6.88 mmol, 0.56 g) and *N*,*N*-diphenylaminobenzaldehyde (3.11 mmol, 0.85 g). One drop of TFA was added and the solution was stirred under N_2 at room temperature for 1 day. After addition of DDQ (3.11 mmol, 0.76 g) to the reaction mixture, stirring was continued for 30 min. 4 mL of Et_3N and 4 mL of $BF_3 \cdot OEt_2$ were successively added and after 30 min, the reaction mixture was washed three times with water (3×100 mL), which was then extracted into the CH_2Cl_2 (3×100 mL) and dried over anhydrous Na_2SO_4. The solvent was evaporated and the residue was purified by silica gel column chromatography using CH_2Cl_2 as the eluent (0.61 g, 31%). ^{1}H NMR (400 MHz, $CDCl_3$): δ=7.39 (d, J=8.82, 2H), 7.37–7.33 (m, 4H), 7.25–7.20 (m, 4H), 7.16 (d, J=7.33, 2H), 7.11 (d, J=8.69, 2H), 6.87 (d, J=4.12, 2H), 6.30 (d, J=4.13, 2H). ^{13}C NMR (100 MHz, $CDCl_3$): δ_C 156.6, 150.0, 146.9, 142.8, 137.0, 134.3, 131.8, 130.1, 129.6, 126.9, 125.6, 124.2, 120.6, 119.0, 14.8 ppm. ESI-MS: m/z: calcd: 463.20313, found: 463.20355 $[M+H]^+$, Δ=0.91 ppm.

*4.3.4. Synthesis of BHJ **2**.* (**2**) (0.31 mmol, 145 mg) and *N*,*N*-diphenylaminobenzaldehyde (0.94 mmol, 257 mg) were added to

a 100 mL round-bottomed flask containing 50 mL benzene and to this solution was added piperidine (0.3 mL) and acetic acid (0.3 mL). The mixture was heated under reflux by using a Dean Stark trap and reaction was monitored by TLC (2:1 EtOAc/Hexane). When all the starting material had been consumed, the mixture was cooled to room temperature and solvent was evaporated. Water (100 mL) added to the residue and the product was extracted into the CH_2Cl_2 (3×100 mL). Organic phase dried over Na_2SO_4, evaporated and residue was purified by silica gel column chromatography using (2:1 EtOAc/Hexane) as the eluant. Black solid (75 mg, %20). ^{1}H NMR (400 MHz, $CDCl_3$): δ=7.75 (d, J=16.20, 2H), 7.51 (d, J=8.72, 4H), 7.48–7.31 (m, 16H), 7.27–7.21 (m, 4H), 7.20–7.10 (m, 20H), 6.95 (d, J=7.56, 4H). ^{13}C NMR (100 MHz, $CDCl_3$): δ_C 154.1, 149.6, 148.6, 147.2, 147.1, 147.0, 138.2, 136.0, 135.6, 131.2, 130.4, 130.3, 129.6, 129.4, 129.1, 129.0, 128.6, 127.5, 125.6, 125.5, 125.1, 124.2, 124.1, 124.0, 123.8, 123.7, 123.6, 123.4, 122.5, 123.3, 120.1, 117.7, 115.8 ppm. ESI-MS: m/z: calcd: 973.41273, found: 973.41590 $[M-H]^+$, Δ=3.25 ppm.

4.4. Electrochemistry of Bodipy dyes

CV measurement was taken by using CH-Instrument 660 B Model Potentiostat equipment. Solution was prepared in chloroform (10^{-3} M). A three-electrodes cell was used consisting of Glassy carbon working electrode, Pt wire counter electrode and Ag/AgCl reference electrode, all placed in a glass vessel. Tetrabutylammonium hexafluorophosphate ($TBAPF_6$), 0.1 M, was used as supporting electrolyte. Ferrocene was used as internal reference electrode. HOMO/LUMO values were calculated according to literature.[18]

4.5. Bulk heterojunction device fabrication

Bulk heterojunction solar cells were fabricated in FTO/PEDOT:PSS/Bodipy:PCBM/Al device configuration. A schematic illustration of bulk heterojunction solar cell configuration is shown in Fig. 1. Bulk heterojunction solar cell devices were prepared according to following procedure. FTO glasses were cut into square plates (2.5×2.5 cm). Fluorine-doped tin oxide (FTO) glasses were patterned by etching with Zn dust and acid solution. All FTO glasses were cleaned with acetone and ethanol for 10 min in ultrasonic bath then with Helmanex soap for 20 min, after that distilled water were used for cleaning, and again ethanol was employed and finally dried by N_2 purging. The Bodipy/PCBM was blended with a 1:2 blend ratio and was dissolved in chlorobenzene. PEDOT:PSS was spincoated on FTO glasses in 1500 rpm. Then Bodipy/PCBM blend was again spincoated on top of PEDOT:PSS layer. Finally, Al electrode was thermally evaporated at 10^{-6} mbar vacuum pressure through a shadow mask in the glove box.

4.6. Bulk heterojunction solar cell device characterization

The current densities versus voltages (I–V) characteristics of the devices were measured with a source measurement unit Keithley 2400. The device performance were characterized under AM 1.5 G condition with an illumination intensity of 100 mW/cm^2 using a solar simulator. A special mask was used to define active area of each finger in the devices and measurements were carried out using this special mask. Reproducibility of measurements was checked for many times for the accuracy and precision.

4.7. Atomic force microscopy (AFM) images

AFM measurements were performed under ambient conditions using a commercial scanning probe microscope in non-contact mode. The AFM topographic images were processed using the XEI program. AFM images were taken using Ambios Atomic Force Microscopy equipment.

Acknowledgements

Y.D. thanks TUBITAK (110T647) for financial support. M.B. thanks TUBITAK for scholarship. We are grateful to TUBITAK ULAKBIM (TR-Grid) and to Gazi University Physics Department (pizag cluster) for computing resources.

Supplementary data

Supplementary data related to this article can be found at http://dx.doi.org/10.1016/j.tet.2014.03.049.

References and notes

1. (a) Yu, G.; Heeger, A. J. *J. Appl. Phys.* **1995**, *78*, 4510; (b) Halls, J. J. M.; Walsh, C. A.; Greenham, N. C.; Marseglia, E. A.; Friend, R. H.; Moratti, S. C. *Nature* **1995**, *376*, 498; (c) Yu, G.; Gao, J.; Hummelen, J. C.; Wudl, F.; Heeger, A. J. *Science* **1995**, *270*, 1789; (d) Gunes, S.; Neugebauer, H.; Sariciftci, N. S. *Chem. Rev.* **2007**, *107*, 1324; (e) Kippelen, B.; Bredas, J.-J. *Energy Environ. Sci.* **2009**, *2*, 251; (f) Thompson, B. C.; Frechet, J. M. F. *Angew. Chem., Int. Ed.* **2008**, *47*, 58; (g) Delgado, J. L.; Bouit, P.-A.; Filippone, S.; Herranz, M. A.; Martin, N. *Chem. Commun.* **2010**, 4853.
2. (a) Brabec, C. J.; Gowrisanker, S.; Halls, J. J. M.; Laird, D.; Jia, S.; Williams, S. P. *Adv. Mater.* **2010**, *22*, 3839; (b) Lu, S.; Jin, T.; Yasuda, T.; Si, W.; Oniwa, K.; Alamry, K. A.; Kosa, S. A.; Asiri, A. M.; Han, L.; Yamamoto, Y. *Org. Lett.* **2013**, *15*, 5674; (c) Lu, S.; Jin, T.; Yasuda, T.; Islam, A.; Akhtaruzzaman, M.; Han, L.; Alamry, K. A.; Kosa, S. A.; Asiri, A. M.; Yamamoto, Y. *Tetrahedron* **2013**, *69*, 1302.
3. (a) Hummelen, J. C.; Knight, B. W.; Lepec, F.; Wudl, F.; Yao, J.; Wilkins, C. L. *J. Org. Chem.* **1995**, *60*, 532; (b) Li, G.; Schrotriya, V.; Huang, J.; Yao, Y.; Moriarty, T.; Emery, K.; Yang, Y. *Nat. Mater.* **2005**, *4*, 864; (c) Park, S. H.; Roy, A.; Beaupre, S.; Cho, S.; Coates, N.; Moon, J. S.; Moses, D.; Leclerc, M.; Lee, K.; Heeger, A. J. *Nat. Photonics* **2009**, *3*, 297; (d) Price, S. C.; Stuart, A. C.; Yang, L.; Zhou, H.; You, W. *J. Am. Chem. Soc.* **2011**, *133*, 4625; (e) Service, F. *Science* **2011**, *332*, 293; (f) Li, Y. *Acc. Chem. Res.* **2012**, *45*, 723.
4. (a) Muhlbacher, D.; Scharber, M.; Morana, M.; Zhu, Z.; Waller, D.; Gaudiana, R.; Brabec, C. *Adv. Mater.* **2006**, *18*, 2884; (b) Brabec, C. J.; Heeney, M.; McCulloch, I.; Nelson, J. *Chem. Soc. Rev.* **2011**, *40*, 1185; (c) Huo, L.; Zhang, S.; Guo, X.; Xu, F.; Li, Y.; Hou, J. *Angew. Chem., Int. Ed.* **2011**, *50*, 9697; (d) Huang, Y.; Guo, X.; Liu, F.; Huo, L.; Chen, Y.; Russell, T. P.; Han, C. C.; Li, Y.; Hou, J. *Adv. Mater.* **2012**, *24*, 3383.
5. (a) Roncali, J.; Leriche, P.; Cravino, A. *Adv. Mater.* **2007**, *19*, 2045; (b) He, C.; He, Q.; Yi, Y.; Wu, G.; Yang, C.; Bai, F.; Shuai, Z.; Wang, L.; Li, Y. *J. Mater. Chem.* **2008**, *18*, 4085; (c) Kroneneberg, N. M.; Deppish, M.; Würthner, F.; Ledemann, H. W. A.; Deing, K.; Meerholz, K. *Chem. Commun.* **2008**, 6489; (d) Zhang, J.; Deng, D.; He, C.; He, Y. J.; Zhang, M. J.; Zhang, Z. G.; Zhang, Z. J.; Li, Y. F. *Chem. Mater.* **2011**, *23*, 817; (e) Wei, G. D.; Wang, S. Y.; Renshaw, K.; Thompson, M. E.; Forrest, S. R. *ACS Nano* **2010**, *4*, 1927; (f) Steinberger, A.; Mishra, A.; Reinold, E.; Levichkov, J.; Uhrich, C.; Pfeiffer, M.; Bäuerle, P. *Chem. Commun.* **2011**, 1982; (g) Sharma, G. D.; Mikroyannidis, J. A.; Kurchania, R.; Thomas, K. R. J. *J. Mater. Chem.* **2012**, *22*, 13986; (h) Qu, S.; Tian, H. *Chem. Commun.* **2012**, 3039; (i) Erten-Ela, S.; Brendel, J.; Thelakkat, M. *Chem. Phys. Lett.* **2011**, *510*, 93; (j) Roncali, J. *Acc. Chem. Res.* **2009**, *42*, 1719; (k) Shen, S.; Jiang, P.; He, C.; Zhang, J.; Shen, P.; Zhang, Y.; Yi, Y.; Zhang, Z.; Li, Z.; Li, Y. *Chem. Mater.* **2013**, *25*, 2274.
6. (a) Ziessel, R.; Ulrich, G.; Harriman, A. *New J. Chem.* **2007**, *31*, 496; (b) Loudet, A.; Burgess, K. *Chem. Rev.* **2007**, *107*, 4891; (c) Ulrich, G.; Ziessel, R.; Harriman, A. *Angew. Chem., Int. Ed.* **2008**, *47*, 1184.
7. Buyuktemiz, M.; Duman, S.; Dede, Y. *J. Phys. Chem. A* **2013**, *117*, 1665.
8. (a) Sunahara, H.; Urano, Y.; Kojima, H.; Nagano, T. *J. Am. Chem. Soc.* **2007**, *129*, 5597; (b) Yin, S. C.; Leen, V.; Van Snick, S.; Boens, N.; Dehaen, W. *Chem. Commun.* **2010**, 6329; (c) Qi, X.; Kim, S. K.; Han, S. J.; Xu, L.; Jee, A. Y.; Kim, H. N.; Lee, C.; Kim, Y.; Lee, M.; Kim, S. J.; Yoon, J. *Tetrahedron Lett.* **2008**, *49*, 261; (d) Niu, S.; Massif, C.; Ulrich, G.; Renard, P.; Romieu, A.; Ziessel, R. *Chem.—Eur. J.* **2012**, *18*, 7229; (e) Rurack, K.; Kollmansberger, M.; Resch-Genger, U.; Daub, J. *J. Am. Chem. Soc.* **2000**, *122*, 968; (f) Isik, M.; Ozdemir, T.; Simsek-Turan, I.; Kolemen, S.; Akkaya, E. U. *Org. Lett.* **2013**, *15*, 216; (g) Niu, L.-Y.; Guan, Y.-S.; Chen, Y.-Z.; Wu, L.-Z.; Tung, C.-H.; Yang, Q.-Z. *J. Am. Chem. Soc.* **2012**, *134*, 18928.
9. (a) Kamkaew, A.; Lim, S. H.; Lee, H. B.; Kiew, L. V.; Chung, L. Y.; Burgess, K. *Chem. Soc. Rev.* **2013**, *42*, 77; (b) Yogo, T.; Urano, Y.; Ishitsuka, F.; Nagano, T. *J. Am. Chem. Soc.* **2005**, *127*, 12162; (c) Gallagher, W. M.; Allen, L. T.; O'Shea, C.; Kenna, T.; Hall, M.; Gorman, A.; Killoran, J.; O'Shea, D. F. *J. Cancer* **2005**, *92*, 1702; (d) Erbas, S.; Gorgulu, A.; Kocakusakogullari, M.; Akkaya, E. U. *Chem. Commun.* **2009**, 4956.
10. (a) Zhang, X.; Xiao, Y.; Qian, X. *Org. Lett.* **2008**, *10*, 29; (b) Bozdemir, O. A.; Cakmak, Y.; Sozmen, F.; Ozdemir, T.; Siemiarczuk, A.; Akkaya, E. U. *Chem.—Eur. J.* **2010**, *16*, 6346; (c) Iehl, J.; Nierengarten, J.-F.; Harriman, A.; Bura, T.; Ziessel, R. *J. Am. Chem. Soc.* **2012**, *143*, 988; (d) Bozdemir, O. A.; Erbas-Cakmak, S.; Ekiz, O. O.; Dana, A.; Akkaya, E. U. *Angew. Chem., Int. Ed.* **2011**, *50*, 10907.

11. (a) Guliyev, R.; Ozturk, S.; Kostereli, Z.; Akkaya, E. U. *Angew. Chem., Int. Ed.* **2011**, *50*, 9826; (b) Erbas-Cakmak, S.; Bozdemir, O. A.; Cakmak, Y.; Akkaya, E. U. *Chem. Sci.* **2013**, *4*, 858.
12. (a) Erten-Ela, S.; Yilmaz, D.; Icli, B.; Dede, Y.; Icli, S.; Akkaya, E. U. *Org. Lett.* **2008**, *10*, 3299; (b) Kumaresan, D.; Thummel, R. P.; Bura, T.; Ulrich, G.; Ziessel, R. *Chem.—Eur. J.* **2009**, *15*, 6335; (c) Lee, C. Y.; Hupp, J. T. *Langmuir* **2010**, *26*, 3760; (d) Kolemen, S.; Bozdemir, O. A.; Cakmak, Y.; Barin, G.; Ertan-Ela, S.; Marszalek, M.; Yum, J. H.; Zakeeruddin, S. M.; Nazeeruddin, M. K.; Grätzel, M.; Akkaya, E. U. *Chem. Sci.* **2011**, *2*, 949.
13. (a) Kolemen, S.; Cakmak, Y.; Erten-Ela, S.; Altay, Y.; Brendel, J.; Thelakkat, M.; Akkaya, E. U. *Org. Lett.* **2010**, *12*, 3812.
14. (a) Rousseau, T.; Cravino, A.; Bura, T.; Ulrich, G.; Ziessel, R.; Roncali, J. *Chem. Commun.* **2009**, 1673; (b) Rousseau, T.; Cravino, A.; Bura, T.; Ulrich, G.; Ziessel, R. *J. Mater. Chem.* **2009**, *19*, 2298; (c) Rousseau, T.; Cravino, A.; Ripaud, E.; Leriche, P.; Rihn, S.; Nicola, A. D.; Ziessel, R.; Roncali, J. *Chem. Commun.* **2010**, 5082; (d) Lin, H.-Y.; Huang, W.-C.; Chou, H.-H.; Hsu, C.-Y.; Lin, J. T.; Lin, H. W. *Chem. Commun.* **2012**, 8913; (e) Kim, B.; Ma, B.; Donuru, V. R.; Liu, H.; Frechet, J. M. J. *Chem. Commun.* **2010**, 4148; (f) Bura, T.; Leclerc, N.; Fall, S.; Leveque, P.; Heiser, T.; Retailleau, P.; Rihn, S.; Mirloup, A.; Ziessel, R. *J. Am. Chem. Soc.* **2012**, *134*, 17404.
15. Buyukcakir, O.; Bozdemir; Kolemen, S.; Erbas, S.; Akkaya, E. U. *Org. Lett.* **2009**, *11*, 4644.
16. Hou, J. H.; Tan, Z. A.; Yan, Y.; He, Y. J.; Yang, C. H.; Li, Y. F. *J. Am. Chem. Soc.* **2006**, *128*, 4911.
17. (a) Kanai, Y.; Grossman, J. C. *Nano Lett.* **2007**, *7*, 1967; (b) Liu, T.; Troisi, A. *J. Phys. Chem. C* **2011**, *115*, 2406.
18. Cowan, D. O.; Drisko, R. L. E. *J. Am. Chem. Soc.* **1970**, *92*, 6281.